Nuclear data in the Cosmos from the Interacting Shell Model

Sofia Karampagia

Celebrating 75 Years of the Nuclear Shell Model and Maria Goeppert-Mayer

Support from NASA grant 80NSSC20M0124, MSGC is acknowledged

Grand Valley State University

The development of the Nuclear Shell Model

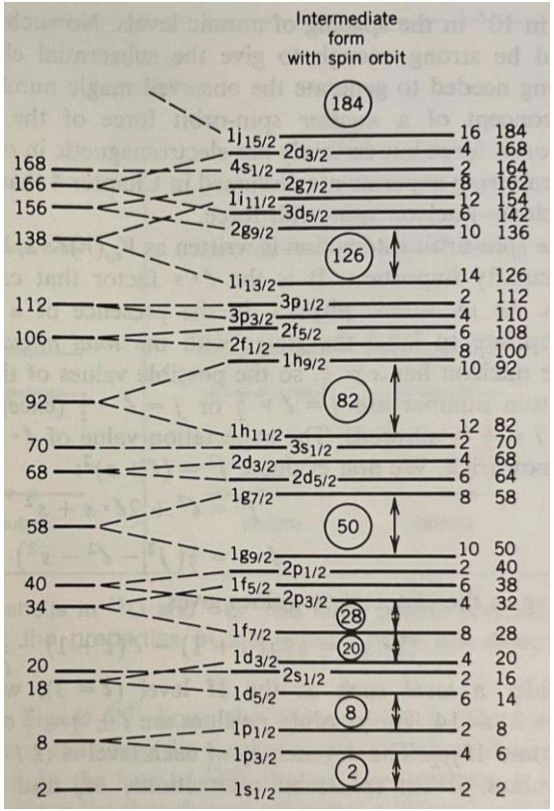

Maria Goeppert-Mayer and Hans Jensen proposed the extreme single particle model: individual nucleons move independently in a mean-field potential.

The “magic numbers” 2, 8, 20, 28, 50, 82, 126, 184 are reproduced after the inclusion of the spin-orbit term.

Mayer, M.G ., Jensen, J.H.D., Elementary Theory of Nuclear Structure New York: Wiley (1955)

The development of the Nuclear Shell Model

Later, the shell model included the interactions between the (valence) nucleons.

$^{20}_{10}Ne$ – sd valence space

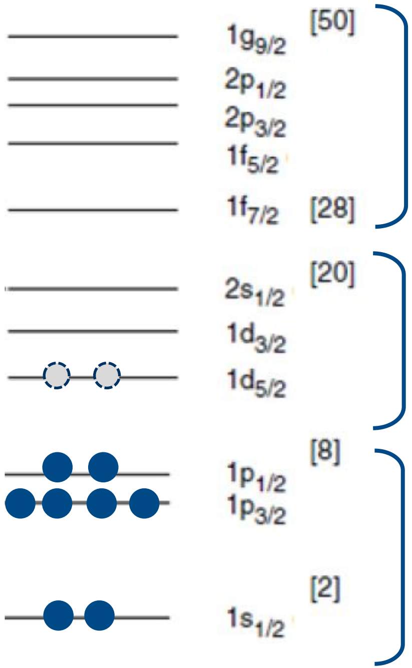

Higher, empty shells (Particles cannot be excited to these shells)

Valence shell

Core (Completely occupied shells)

Traditionally, the effective interaction for the valence space has been obtained by either fitting the TBME to selected experimental spectra or G-matrices obtained by a bare NN potential with core polarization corrections.

More methods of deriving shell model Hamiltonians have been developed and will be presented at the symposium, as well recent developments in no-core shell model and ab-initio methods.

Grand Valley State University

Nuclear reaction processes responsible for the synthesis of elements

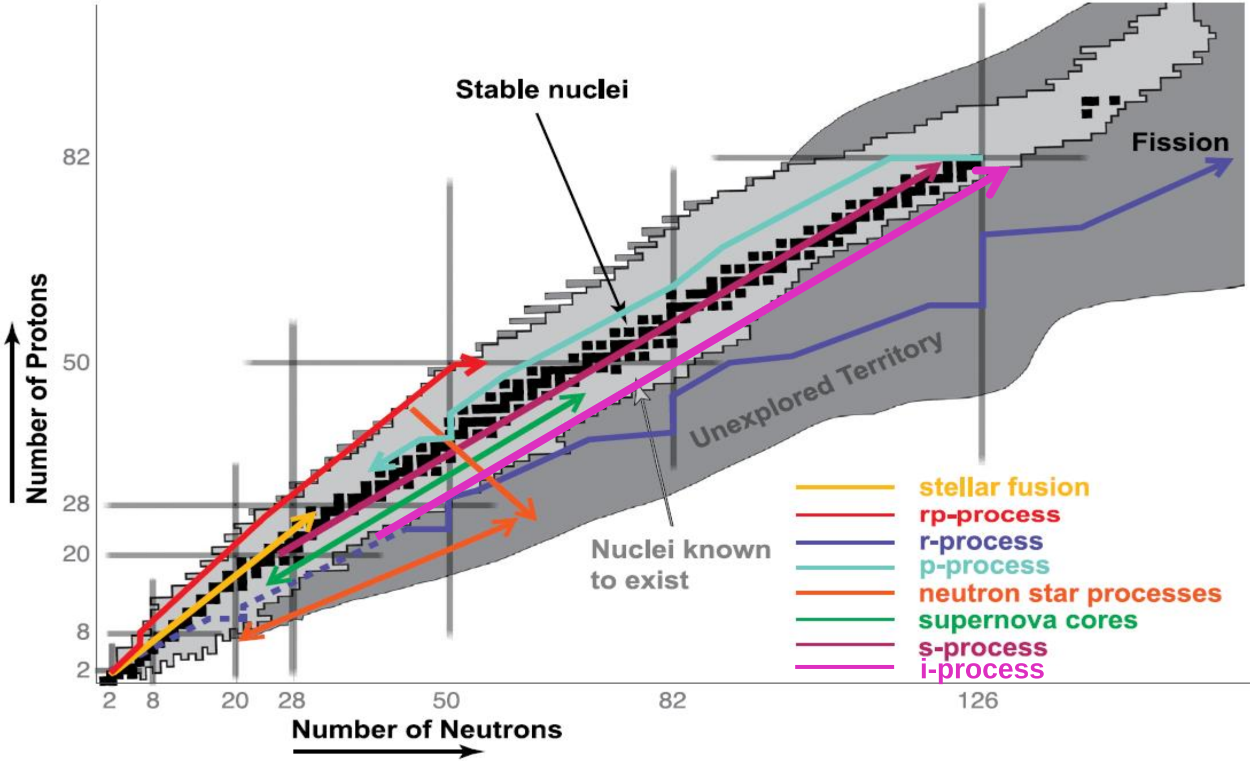

Elements rich in neutrons:
neutron capture nucleosynthesis, competition between neutron capture reactions and β decays.

Elements rich in protons:
proton/alpha captures
photodisintegration
proton capture/neutron induced reactions

A. Arcones *et al*. PPNP 94, 1 (2017)

Solar abundance distributions for heavy-element isotopes

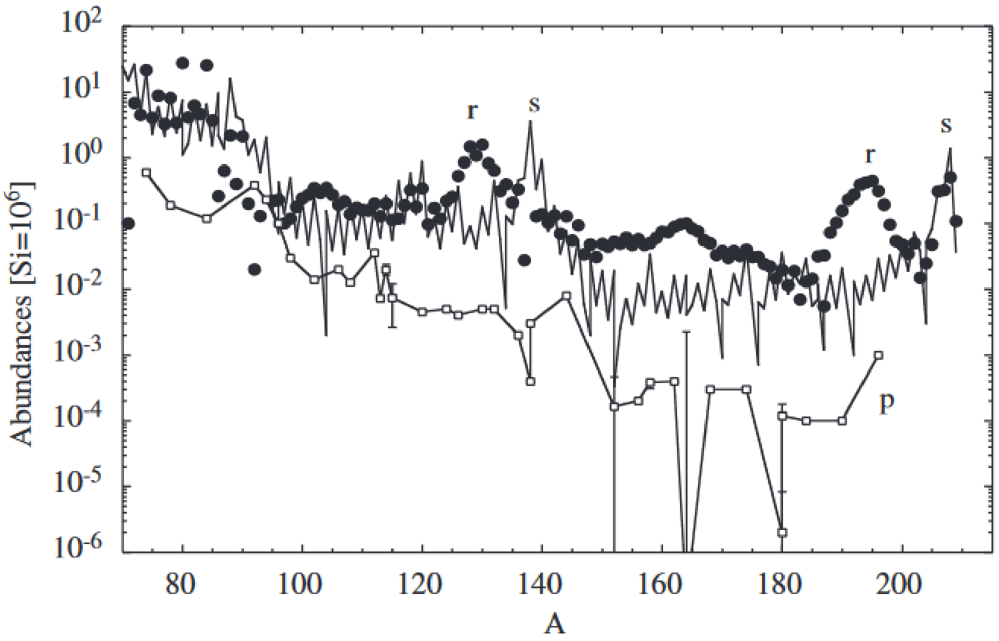

- Simulations of elemental abundance distributions are obtained through nucleosynthesis reaction network codes.
- Astrophysical conditions of the site where the nucleosynthesis occurs.
- Nuclear properties of participating nuclei. (For instance, peaks in the abundance distribution correlated to neutron shell closures.)

r-process

- r-process: Responsible for the production of half of the elements heavier than iron, proceeding via successive neutron captures and beta decays.
- Identifying the astrophysical sites of the r-process remains challenging. Modeling the r-process abundance distribution is subject to uncertainties stemming from the challenges modeling these astrophysical environments.
- Early r-process, high temperatures, statistical equilibrium between neutron capture and dissociation reactions. Neutron separation energies, determined by nuclear masses are important in that phase.
- When the available free neutrons are drastically reduced, the statistical equilibrium fails. The competition between neutron captures, photodissociation and β-decay makes neutron capture rates important.

Neutron Capture rates within the statistical Hauser-Feshbach model

- For nuclei participating in the r-process the experimental derivation of neutron capture rates is not possible. Neutron capture rates are predicted theoretically through the Hauser-Feshbach statistical model. (Neutron and target combine to form a compound system which subsequently decays by emitting γ-rays.)
- Main ingredients for neutron capture rate calculations within the statistical Hauser-Feshbach approach:
  - Nuclear Level Densities
  - γ-strength functions (γSF)
  - Optical model potentials
- Hauser-Feshbach approach not applicable for low neutron capture Q values.

Impact of NLDs, γSF in neutron capture rates

Variations of neutron capture rates at 1.5 GK

Nuclear Level Density	γ ray Strength Function
Constant Temperature matched to the Fermi Gas model (CT+BSFG)[19]	Kopecky-Uhl generalized Lorentzian (KU) [17]
Back-shifted Fermi Gas model (BSFG)[19],[20]	Hartree-Fock BCS + QRPA (HF-BCS+QRPA) [21]
Generalized Super fluid model (GSM)[22], [23]	Hartree-Fock-Bogolyubov + QRPA (HFB+QRPA) [24]
Hartree Fock using Skyrme force (HFS) [25]	Modified Lorentzian (Gor-ML)[26]
Hartree-Fock-Bogoliubov (Skyrme force) + combinatorial method (HFBS-C) [27]	

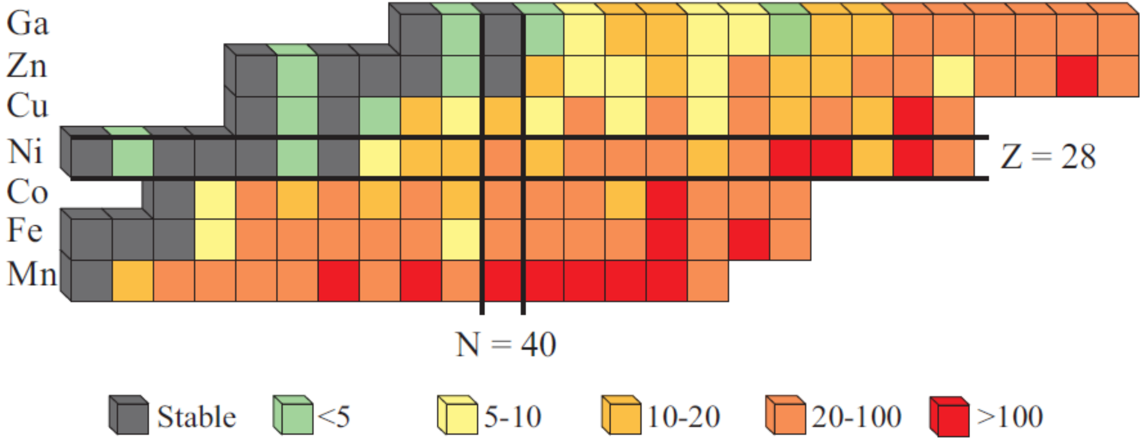

S. N. Liddick *et al*. PRL 116, 242502 (2016)

γ-ray strength function

Low energy enhancement

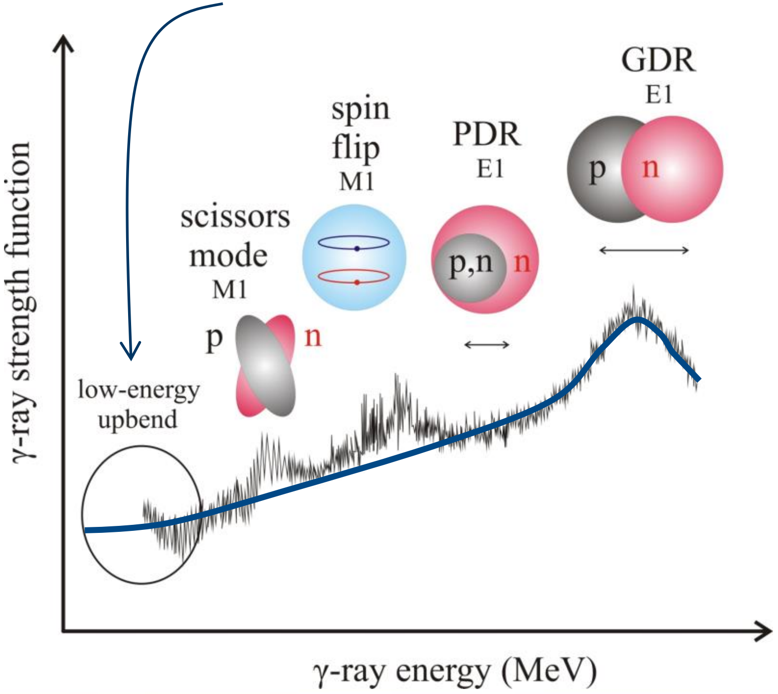

The γSF describes the average energy distribution of γ-rays emanating from high energy states of the nucleus.

Generalized Lorentzian (GLO)

$$f_{GLO} = \frac{1}{3\pi^2\hbar^2c^2}\sigma_{\mathrm{E1}}\Gamma_{\mathrm{E1}}$$

$$\times\left[\frac{E_\gamma \Gamma(E_\gamma, T)}{\left(E_\gamma^2 - \mathrm{E}_{\mathrm{E1}}^2\right)^2 + E_\gamma^2 \Gamma(E_\gamma, T)^2} + 0.7\frac{\Gamma(E_\gamma = 0, T)}{E_{\mathrm{E1}}^3}\right]$$

$$\Gamma(E_\gamma, T) = \frac{\Gamma_{\mathrm{E1}}}{E_{\mathrm{E1}}^2}\left(E_\gamma^2 + 4\pi^2T^2\right)$$

Impact on (n,γ) reaction rates

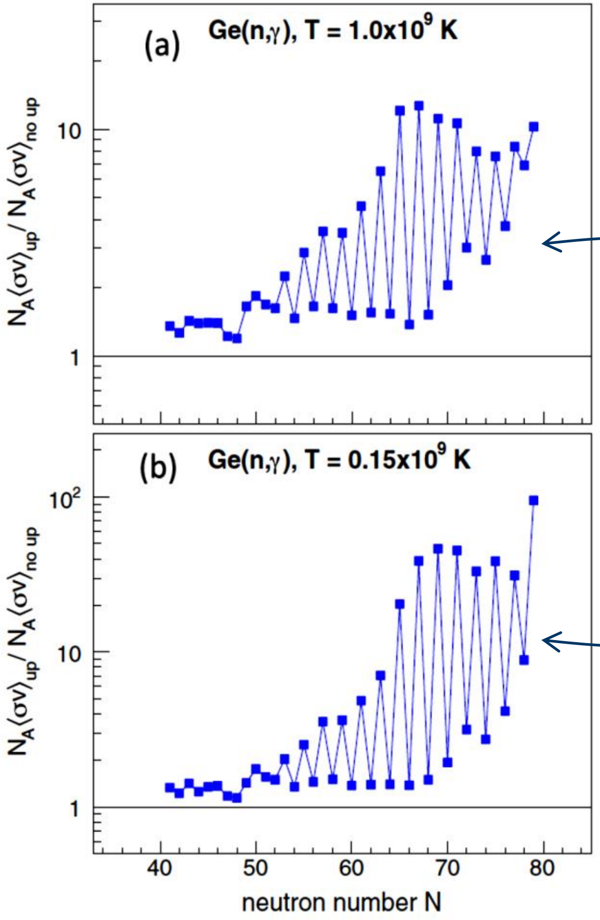

$$f_{up}(E_\gamma) = Cexp[-\eta E_\gamma]$$
$$(C, \eta) = (4 \times 10^{-8}, 0.99)$$

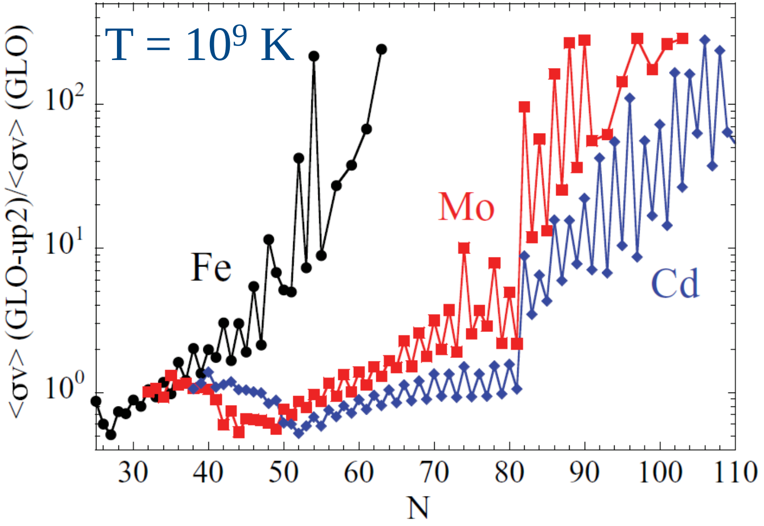

The γSF low energy enhancement becomes increasingly important as the number of neutrons increases.

Configuration-interaction shell model calculations using effective interactions show an **M1 contribution** to the low-energy enhancement.

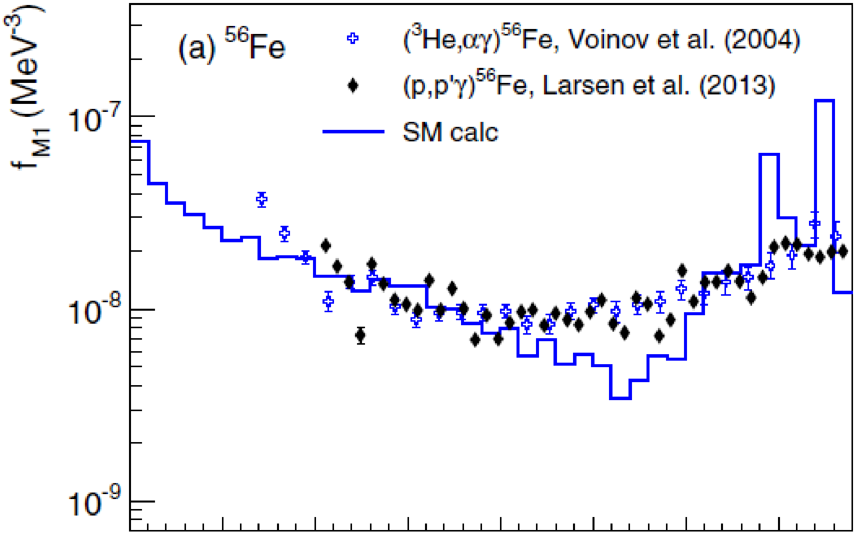

pf shell, GX1A effective interaction

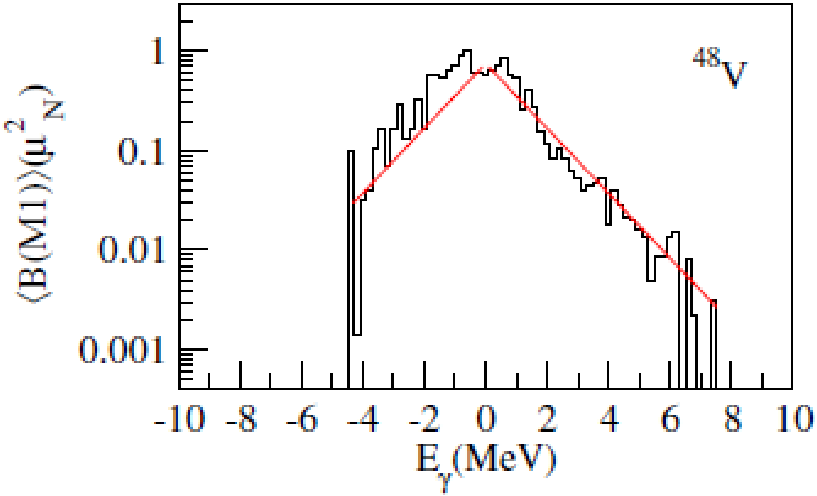

$f_{7/2}$ shell, F742 effective interaction

B. A. Brown *et al*, PRL 113, 252502 (2014)

S. Karampagia *et al*, PRC 95, 024322 (2017)

Configuration-interaction shell model calculations using effective interactions and recent calculations using the Shell model Monte Carlo method show a reduction in the **M1** low energy enhancement with increasing neutron number as another peak emerges, at the location of scissors mode resonance.

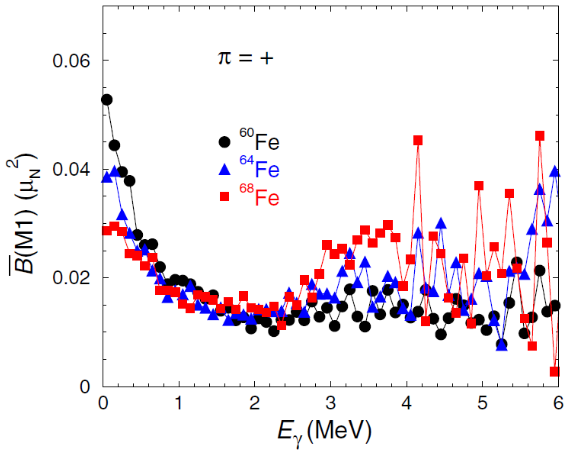

CA48PN shell, CA48MH1 effective interaction

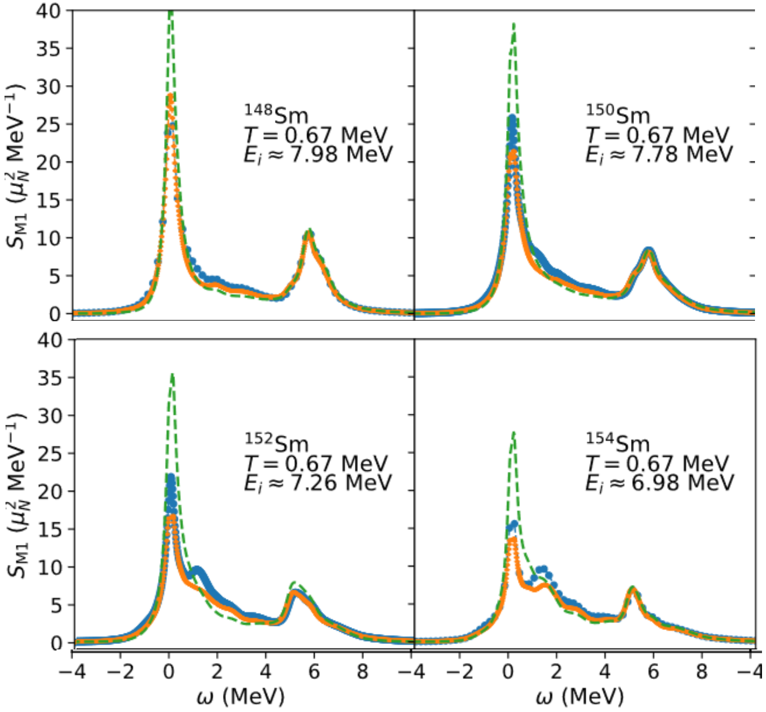

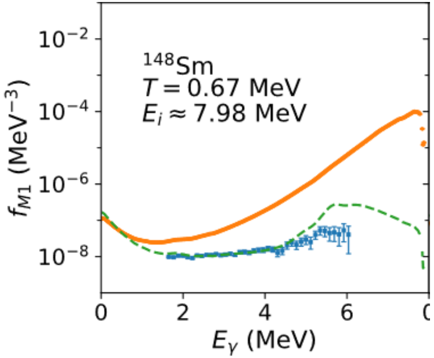

Nuclear level densities (NLD)

Definition: number of levels per energy interval

Experimental NLDs

- Low energy discrete experimental levels
- Level density from neutron resonance spacings at the neutron separation energy (available only for specific spins)
- Spin distribution: $f(J,\sigma) = \frac{2J+1}{2\sigma^2} e^{-\frac{J(J+1)}{2\sigma^2}}$, σ: spin cut-off parameter
- Oslo method and β-Oslo technique
- Particle evaporation from compound nuclear reactions

A. Schiller *et al*, N. Inst. Meth. Phys. Res., Sect. A 447, 498 (2000).

A. C. Larsen et al, Nuclei in the Cosmos XV. Springer Proc. in Phys., vol 219. Springer.

H. Vonach,, BNL Report No. BNL-NCS-51694, p. 247.

NLD Models in Hauser-Feshbach codes

- Phenomenological: Fermi gas model, Constant temperature model, Model parameters must be determined from the available experimental data or from empirical expressions, knowledge of the spin distribution and spin cut-off parameter σ is required
- Microscopic models: built on combinatorics and the HFB model

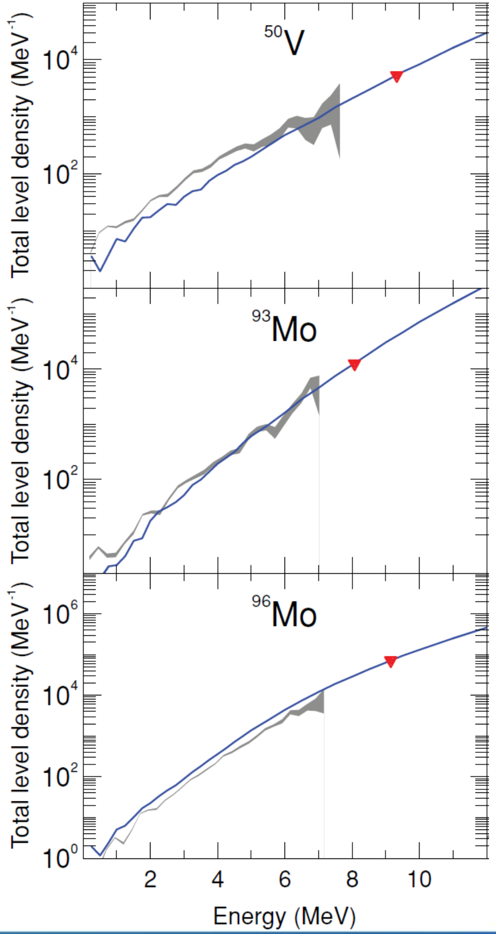

H. A. Bethe, PR 50 332 (1936) A. Gilbert et al., CJP 43 1248 (1965) T. Ericson, Adv Phys 9 425 (1960)
S. Goriely et al., PRC 78 064307 (2008) S. Hilaire et al., PRC 86 064317 (2012)

NLDs from Shell model

- NLDs from configuration interaction shell model calculations using conventional diagonalization are only possible in the sd-shell.
- Shell Model Monte Carlo; mid-mass and heavy nuclei

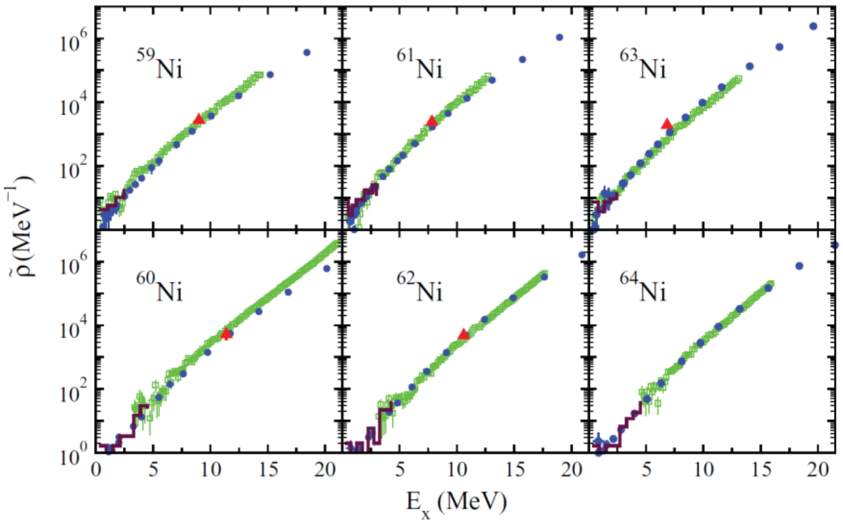

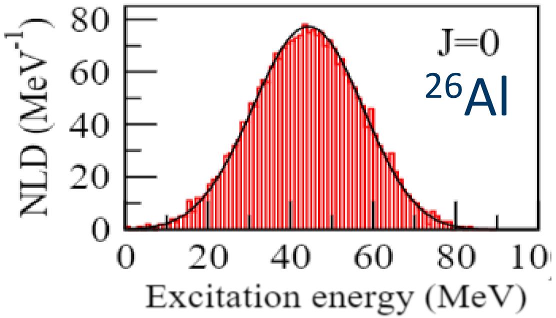

Moments method – based on the CI shell model

Computation of the first two moments of the Hamiltonian; does not require the diagonalization of the involved matrices

The calculated NLD of each proton/neutron configuration is assumed to be a gaussian.

Partitions, p

p	$d_{5/2}$	$s_{1/2}$	$d_{3/2}$
1	6	0	0
2	5	1	0
3	5	0	1
4	4	2	0
...	...	...	...
15	0	2	4

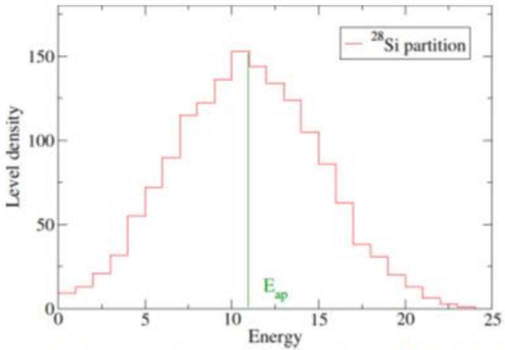

Each partition p, gives a gaussian distribution

$$E_{ap} = \frac{1}{D_{ap}} Tr^{ap} H$$

$$\sigma_{ap}^2 = \frac{1}{D_{ap}} Tr^{ap} H^2 - E_{ap}^2$$

$$G_{ap} = G(E - E_{ap} + E_{g.s}; \sigma_{ap})$$

$$G(x;\sigma) = C \begin{cases} e^{-x^2/2\sigma^2}, & |x| \leq \eta\sigma, \\ 0, & |x| > \eta\sigma \end{cases}$$

$E_{g.s.}$: Shell model

η : cut-off (2.8)

$$\rho(E;a) = \sum_p D_{ap} G_{ap}(E)$$

R. Sen'kov et al., CPC 184, 215 (2013)

Moments method – comparison with experimental/theoretical NLDs

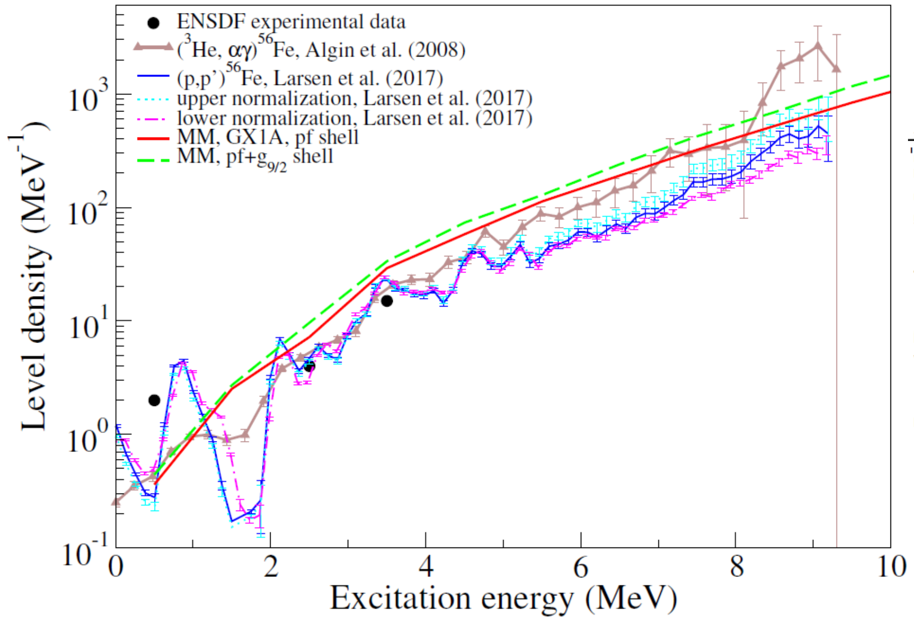

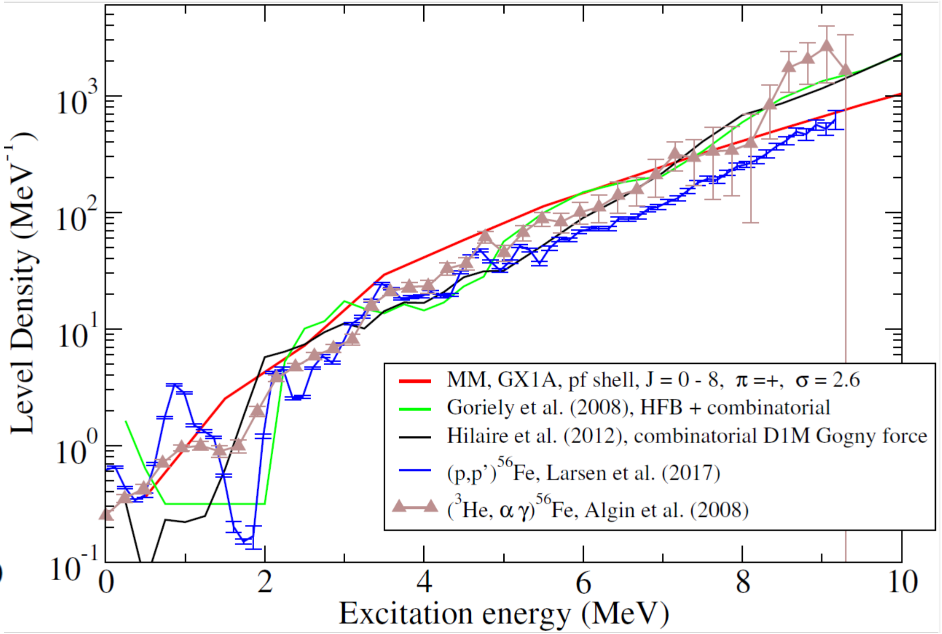

R. Sen'kov et al., CPC 184, 215 (2013)

Astrophysical reaction rates – Moments Method - TALYS

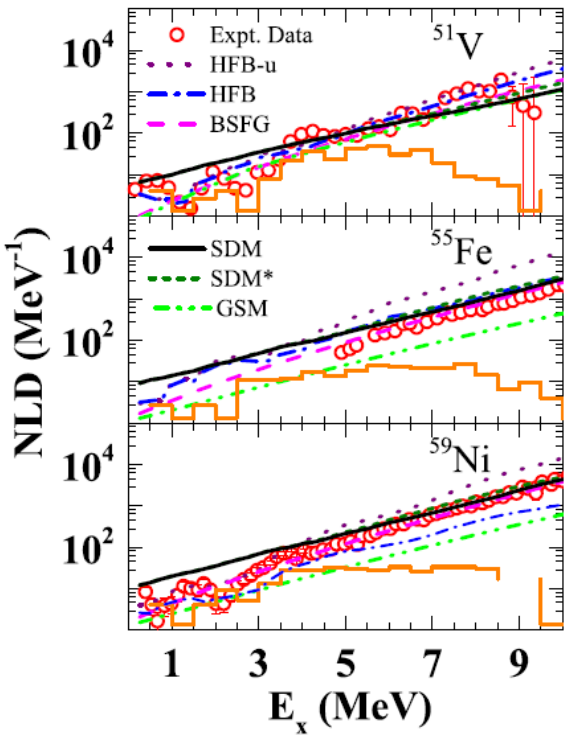

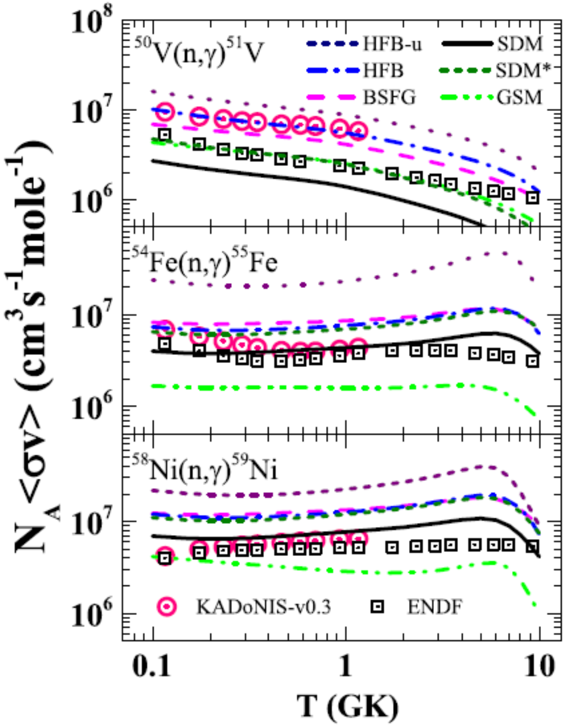

Moments method calculations in pf model space.

Comparison between different NLD models in TALYS.

Sangeeta et al., PRC 105, 044320 (2022)

Challenges

- Shell model level densities have a finite excitation range (~12 MeV); need for an algorithm to continue to higher excitation energies
- Negative/positive parity levels
- Ground state is required; directly from a shell model calculation, other extrapolation techniques
- Availability of reliable shell model interactions (away from stability what?)

Thank you

Model spaces

•Any model space for which **an effective shell model Hamiltonian is available**

Tested with

- *sd* – $0d_{5/2}, 0d_{3/2}, 1s_{1/2}$
- *pf* – $0f_{7/2}, 0f_{5/2}, 1p_{3/2}, 1p_{1/2}$
- *jj44* – $0f_{5/2}, 1p_{3/2}, 1p_{1/2}, 0g_{9/2}$
- *pf* + $0g_{9/2}$

Extensions

– *jj55* – $0g_{7/2}, 1d_{5/2}, 1d_{3/2}, 2s_{1/2}, 0h_{11/2}$

…

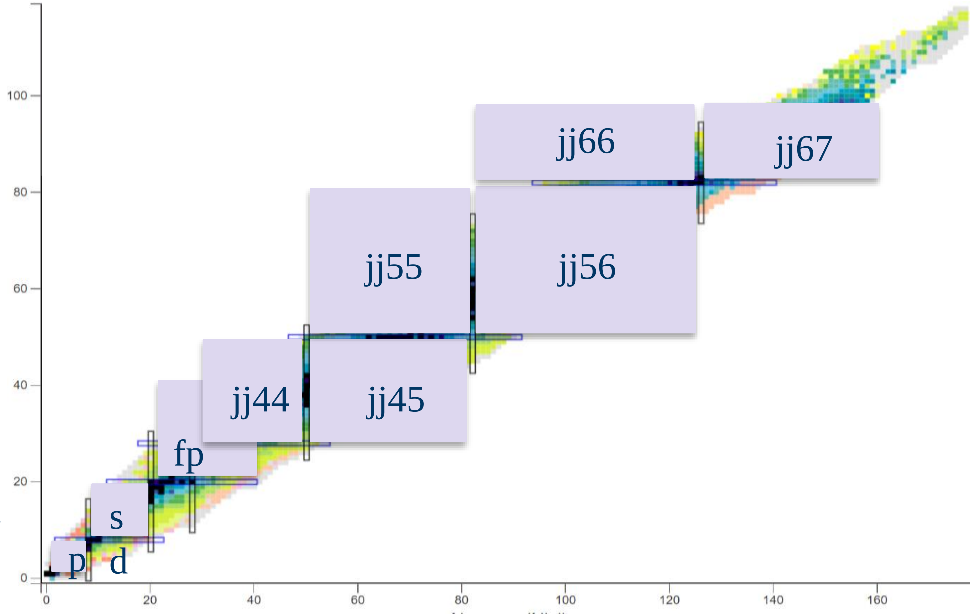

MM vs Exact SM calculations NLDs

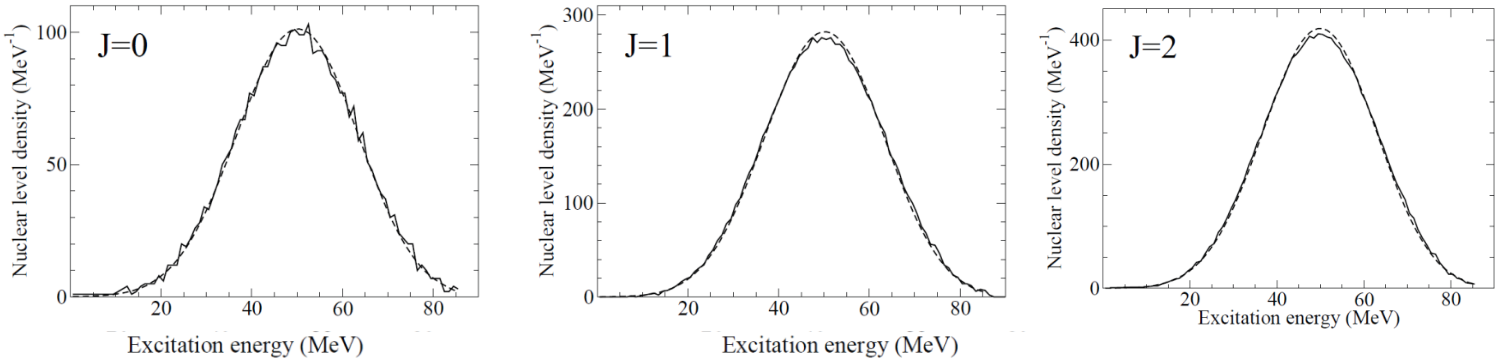

sd – ^{28}Si

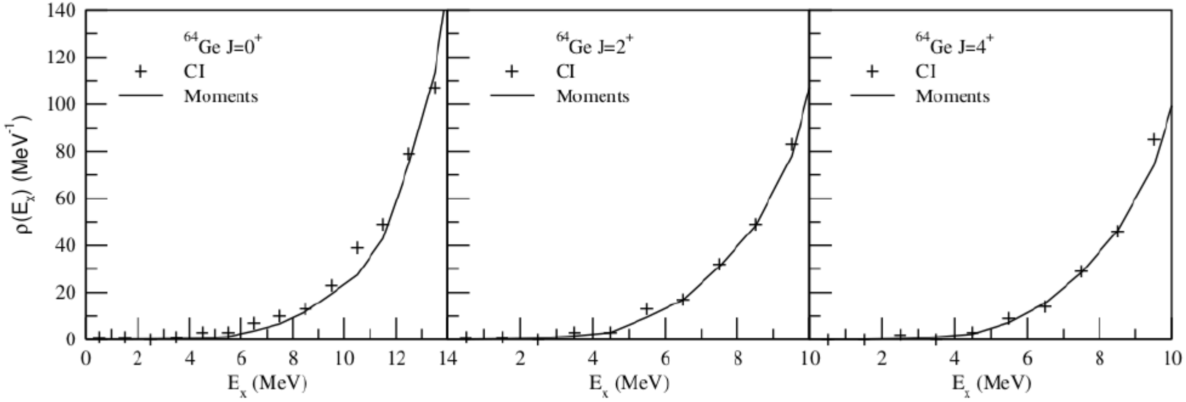

jj44 – ^{64}Ge

R. Sen'kov et al., PRC 93 064304 (2016), M. Scott et al., PoS (2008)

MM vs Experimental NLDs

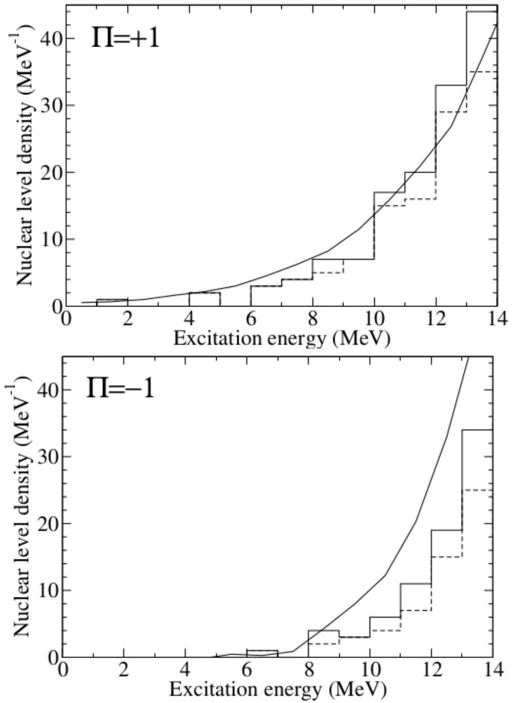

s + p + sd +pf – ^{28}Si

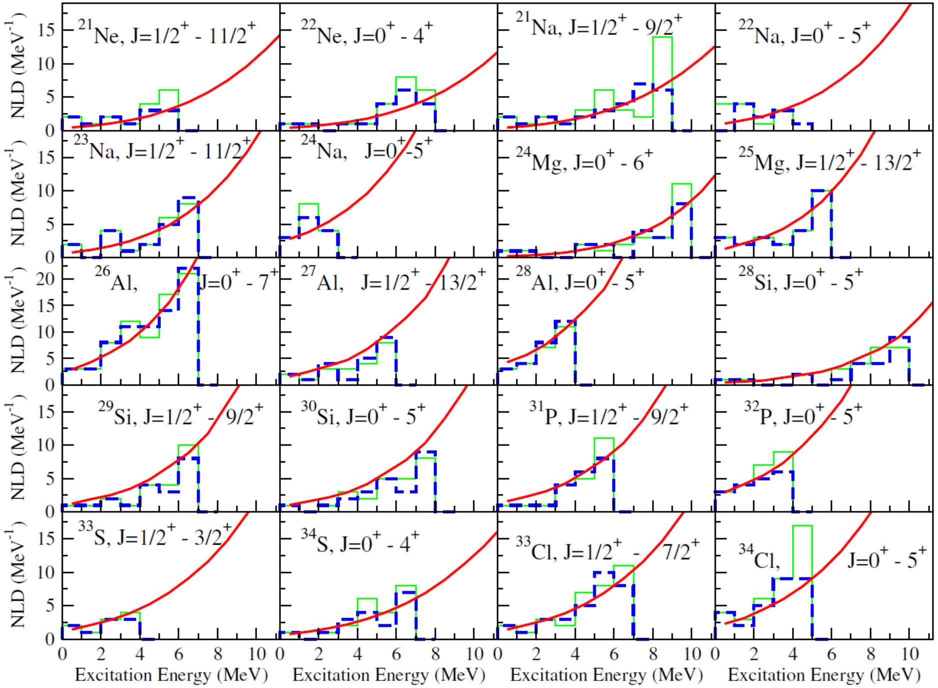

sd – positive parity

R. Sen'kov et al., PRC 93 064304 (2016)

S. Karampagia et al., ADNT 1, 120 (2017)

MM vs other models & Oslo method

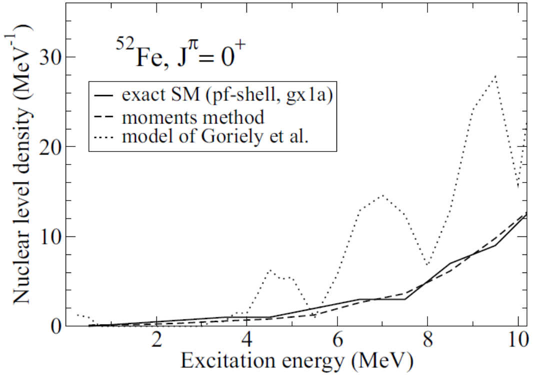

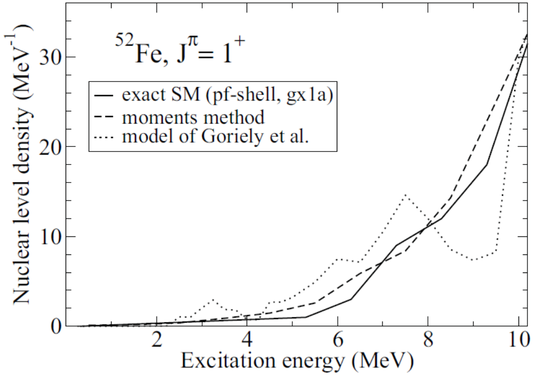

pf – ^{52}Fe

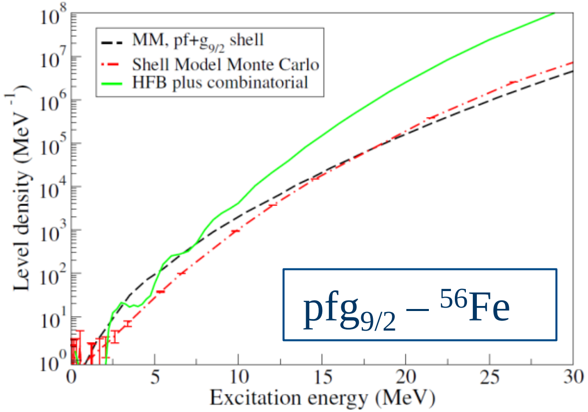

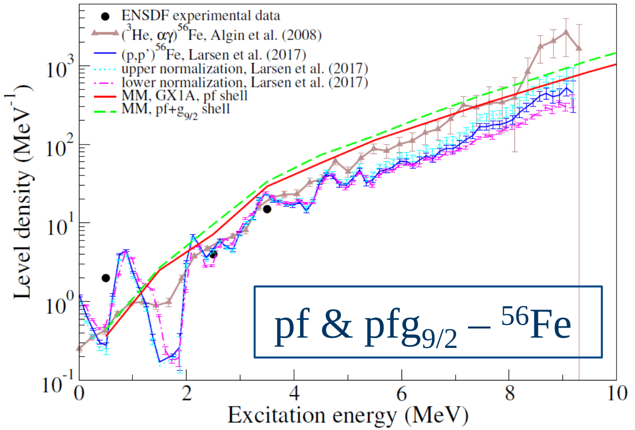

R. Sen'kov et al., PRC 82 024304 (2010)
S. Goriely et al., PRC 78 064307 (2008)